

---

---

ORDER, DISORDER, AND PHASE TRANSITION  
IN CONDENSED SYSTEM

---

---

## Temperature Dependence of the Upper Critical Field in Disordered Hubbard Model with Attraction<sup>1</sup>

E. Z. Kuchinskii<sup>a,\*</sup>, N. A. Kuleeva<sup>a</sup>, and M. V. Sadovskii<sup>a,b,\*\*</sup>

<sup>a</sup> Institute for Electrophysics, Russian Academy of Sciences, Ural Branch, Yekaterinburg, 620016 Russia

<sup>b</sup> Mikheev Institute for Metal Physics, Russian Academy of Sciences, Ural Branch, Yekaterinburg, 620108 Russia

\* e-mail: kuchinsk@iep.uran.ru

\*\* e-mail: sadovski@iep.uran.ru

Received August 30, 2017

**Abstract**—We study disorder effects upon the temperature behavior of the upper critical magnetic field in an attractive Hubbard model within the generalized DMFT+ $\Sigma$  approach. We consider the wide range of attraction potentials  $U$ —from the weak coupling limit, where superconductivity is described by BCS model, up to the strong coupling limit, where superconducting transition is related to Bose–Einstein condensation (BEC) of compact Cooper pairs, formed at temperatures significantly higher than superconducting transition temperature, as well as the wide range of disorder—from weak to strong, when the system is in the vicinity of Anderson transition. The growth of coupling strength leads to the rapid growth of  $H_{c2}(T)$ , especially at low temperatures. In BEC limit and in the region of BCS–BEC crossover  $H_{c2}(T)$ , dependence becomes practically linear. Disorder also leads to the general growth of  $H_{c2}(T)$ . In BCS limit of weak coupling increasing disorder lead both to the growth of the slope of the upper critical field in the vicinity of the transition point and to the increase of  $H_{c2}(T)$  in the low temperature region. In the limit of strong disorder in the vicinity of the Anderson transition localization corrections lead to the additional growth of  $H_{c2}(T)$  at low temperatures, so that the  $H_{c2}(T)$  dependence becomes concave. In BCS–BEC crossover region and in BEC limit disorder only slightly influences the slope of the upper critical field close to  $T_c$ . However, in the low temperature region  $H_{c2}(T)$  may significantly grow with disorder in the vicinity of the Anderson transition, where localization corrections notably increase  $H_{c2}(T=0)$  also making  $H_{c2}(T)$  dependence concave.

DOI: 10.1134/S1063776117120159

### INTRODUCTION

The studies of disorder influence on superconductivity have a rather long history. In pioneer papers by Abrikosov and Gor'kov [1–4] they analyzed the limit of weak disorder ( $p_F l \gg 1$ , where  $p_F$  is the Fermi momentum and  $l$  is the mean free path) and weak coupling superconductivity, which is well described by BCS theory. The well-known “Anderson theorem” on the critical temperature  $T_c$  of superconductors with “normal” (nonmagnetic) disorder [5, 6] is usually also attributed to this limit.

The generalization of the theory of “dirty” superconductors for the case of strong enough disorder ( $p_F l \sim 1$ ) (and up to the region of Anderson transition) was done in [7–10], where superconductivity was also analyzed in the weak coupling limit.

Most dramatically, the effects of disordering are reflected in the behavior of the upper critical magnetic field. In the theory of “dirty” superconductors the growth of disorder leads to the increase both of the

slope of the temperature dependence of the upper critical field at  $T_c$  [6] and of  $H_{c2}(T)$  in the whole temperature region [11]. The effects of Anderson localization in the limit of strong enough disorder are also mostly reflected in the temperature dependence of the upper critical field. At the point of the Anderson metal–insulator transition itself, localization effects lead to a rather sharp increase of  $H_{c2}$  at low temperatures and temperature dependence of  $H_{c2}(T)$  is qualitatively different from the dependence derived by Werthamer, Helfand and Hohenberg (WHH) [11], which is characteristic for the theory of “dirty” superconductors, and the  $H_{c2}(T)$  dependence becomes concave, i.e., demonstrates positive curvature [7–9].

The problem of the generalization of BCS theory into the strong coupling region has been known for a pretty long time. Significant progress in this direction was achieved in a paper by Nozieres and Schmitt–Rink [12], who proposed an effective method to study the crossover from BCS–like behavior in the weak coupling region towards Bose–Einstein condensation (BEC) in the strong coupling region. At the same time, the problem of superconductivity of disordered

<sup>1</sup> The article was translated by the authors.

systems in the limit of strong coupling and in BCS–BEC crossover region is still rather poorly developed.

One of the simplest models to study BCS–BEC crossover is the Hubbard model with attractive interaction. The most successful approach to the Hubbard model, both to describe strongly correlated systems in the case of repulsive interaction, as well as to study the BCS–BEC crossover for the case of attraction, is the dynamical mean field theory (DMFT) [13–15].

In recent years, we have developed the generalized DMFT+ $\Sigma$  approach to the Hubbard model [16–21], which is very convenient for the studies of different external (with respect to those accounted by DMFT) interactions. In particular, this approach is well suited for the analysis of two-particle properties, such as optical (dynamic) conductivity [20, 22].

In [23] we have used this approach to analyze single-particle properties of the normal phase and optical conductivity in attractive Hubbard model. This was followed by our use of DMFT+ $\Sigma$  in [24] to study disorder influence on the temperature of superconducting transition, which was calculated within Nozières–Schmitt-Rink approach. In particular, in this work for the case of semi-elliptic “bare” density of states (adequate for three-dimensional case) we have numerically demonstrated the validity of the generalized Anderson theorem, so that all effects of disordering on the critical temperature (for all values of interaction parameter) are related only to general widening of the “bare” band (density of states) by disorder.

An analytic proof of this universality of disorder influence on all single-particle properties in DMFT+ $\Sigma$  approximation and on superconducting critical temperature for the case of a semi-elliptic band was given in [25].

Starting with the classic work by Gor’kov [3], it is well known that the Ginzburg–Landau expansion is of fundamental importance for the theory of “dirty” superconductors, allowing the effective studies of the behavior of various physical parameters close to superconducting critical temperature for different disorder levels [6]. The generalization of this theory (for weak coupling superconductors) to the region of strong disorder (up to the Anderson metal–insulator transition) was done in [7–9].

In [26–28] combining Nozières–Schmitt-Rink approximation with DMFT+ $\Sigma$  for attractive Hubbard models we provided microscopic derivation of the coefficients of Ginzburg–Landau expansion taking into account disordering, which allowed the generalization of Ginzburg–Landau theory to BCS–BEC crossover region and BEC limit of very strong coupling for different levels of disorder. In particular, in [28] using the generalization of self-consistent theory of localization this approach was extended to the case of strong disorder, where Anderson localization effects become important. It was shown, that in the weak coupling limit the slope of the  $H_{c2}(T)$  dependence at

$T = T_c$  increases with disordering in the region of weak disorder in accordance with the theory of “dirty” superconductors, while in the limit of strong disorder localization effects lead to the additional increase of the slope of the upper critical field. However, in the region of BCS–BEC crossover and in BEC limit the slope of  $H_{c2}(T)$  close to  $T_c$  only slightly increases with the growth of disorder and the account of localization effects is more or less irrelevant.

In the present paper, using the combination of Nozières–Schmitt-Rink and DMFT+ $\Sigma$  approximations for the attractive Hubbard model we shall analyze disorder effects on the complete temperature dependence of  $H_{c2}(T)$  for the wide range of  $U$  interaction values, including the region of BCS–BEC crossover, and the wide range of disorder levels up to the vicinity of the Anderson transition.

### HUBBARD MODEL WITHIN DMFT+ $\Sigma$ APPROACH IN NOZIERES–SCHMITT-RINK APPROXIMATION

We consider the disordered nonmagnetic Anderson–Hubbard model with attraction described by the Hamiltonian:

$$H = -t \sum_{\langle ij \rangle \sigma} a_{i\sigma}^\dagger a_{j\sigma} + \sum_{i\sigma} \epsilon_i n_{i\sigma} - U \sum_i n_{i\uparrow} n_{i\downarrow}, \quad (1)$$

where  $t > 0$  is a transfer integral between nearest neighbors,  $U$  is the Hubbard attraction on the lattice site,  $n_{i\sigma} = a_{i\sigma}^\dagger a_{i\sigma}$ —number of electrons operator on the site,  $a_{i\sigma}$  ( $a_{i\sigma}^\dagger$ )—annihilation (creation) operator for an electron with spin  $\sigma$ , and local energies  $\epsilon_i$  are assumed to be independent random variables on different lattice sites. For the validity of the standard “impurity” diagram technique [29, 30] we assume the Gaussian distribution for energy levels  $\epsilon_i$ :

$$\mathcal{P}(\epsilon_i) = \frac{1}{\sqrt{2\pi}\Delta} \exp\left(-\frac{\epsilon_i^2}{2\Delta^2}\right) \quad (2)$$

Distribution width  $\Delta$  serves as a measure of disorder and the Gaussian random field of energy levels (independent on different lattice sites—“white noise” correlations) induces the “impurity” scattering, which is considered within the standard approach, based on calculations of the averaged Green’s functions [30].

The generalized DMFT+ $\Sigma$  approach [16–19] extends the standard dynamical mean field theory (DMFT) [13–15] by addition of an “external” self-energy (SE)  $\Sigma_p(\epsilon)$  (in general case momentum dependent), which is related to any interaction outside the limits of DMFT, and provides an effective method of calculations for both single-particle and two-particle properties [20, 22]. It completely conserves the standard self-consistent equations of DMFT [13–15], while at each step of DMFT iteration procedure the

external SE  $\Sigma_p(\epsilon)$  is recalculated again using some approximate scheme, corresponding to the form of an external interaction and the local Green's function of DMFT is also "dressed" by  $\Sigma_p(\epsilon)$  at each stage of the standard DMFT procedure.

In our problem of scattering by disorder [20, 21] for the "external" SE, entering the DMFT+ $\Sigma$  cycle, we use the simplest (self-consistent Born) approximation neglecting "crossing" diagrams for impurity scattering. This "external" SE remains momentum independent (local).

To solve the effective single-impurity Anderson model of DMFT in this paper, as in our previous works, we use the very efficient method of numerical renormalization group (NRG) [31].

In the following we assume the "bare" band with semi-elliptic density of states (per unit cell with lattice parameter  $a$  and for single spin projection), which is reasonable approximation for three-dimensional case:

$$N_0(\epsilon) = \frac{2}{\pi D^2} \sqrt{D^2 - \epsilon^2}, \quad (3)$$

where  $D$  defines conduction band half-width.

In [25] we have shown that in DMFT+ $\Sigma$  approach for the model with semi-elliptic density of states all the influence of disorder on single-particle properties reduces simply to disorder induced band widening, i.e., to the replacement  $D \rightarrow D_{\text{eff}}$ , where  $D_{\text{eff}}$  is the effective band half-width of conduction band in the absence of correlations ( $U = 0$ ), widened by disorder:

$$D_{\text{eff}} = D \sqrt{1 + 4 \frac{\Delta^2}{D^2}}. \quad (4)$$

The "bare" (in the absence of  $U$ ) density of states, "dressed" by disorder,

$$\tilde{N}_0(\xi) = \frac{2}{\pi D_{\text{eff}}^2} \sqrt{D_{\text{eff}}^2 - \xi^2}, \quad (5)$$

remains semi-elliptic also in the presence of disorder.

It should be noted that in other models of "bare" band disorder induces not only widening of the band, but also changes the form of the density of states. Thus, in the general case there will be no complete universality of disorder influence on single-particle properties, which are reduced to the simple replacement  $D \rightarrow D_{\text{eff}}$ . However, in the limit of strong disorder, which is of primary interest to us, the "bare" band always becomes, in practice, semi-elliptic and the universality is restored [25].

All calculations in this work, as in the previous, were done for rather typical case of a quarter-filled band (number of electrons per lattice site  $n = 0.5$ ).

To analyze superconductivity for a wide range of pairing interaction  $U$ , following [23, 25], we use Nozieres–Schmitt-Rink approximation [12], which allows qualitatively correct (though approximate) description of BCS–BEC crossover region. In this

approach, to determine the critical temperature  $T_c$  we use [25] the usual BCS-like equation:

$$1 = \frac{U}{2} \int_{-\infty}^{\infty} d\epsilon \tilde{N}_0(\epsilon) \frac{\tanh((\epsilon - \mu)/2T_c)}{\epsilon - \mu}, \quad (6)$$

where the chemical potential  $\mu$  for different values of  $U$  and  $\Delta$  is determined from DMFT+ $\Sigma$ -calculations, i.e., from the standard equation for the number of electrons (band filling), which allows us to find  $T_c$  for the wide interval of model parameters, including the BCS–BEC crossover region and the limit of strong coupling, as well as for different levels of disorder. This reflects the physical meaning of Nozieres–Schmitt-Rink approximation: in the weak coupling region transition temperature is controlled by the equation for Cooper instability (6), while in the limit of strong coupling it is determined as BEC temperature controlled by chemical potential.

It was shown in [25], that disorder influence on the critical temperature  $T_c$  and single-particle characteristics (e.g. density of states) in the model with semi-elliptic density of states is universal and reduces only to the change of the effective bandwidth. In the weak coupling region the temperature of superconducting transition is well described by the BCS model, while in the strong coupling region the critical temperature is mainly determined by the condition of Bose–Einstein condensation of Cooper pairs and decreases with the growth of  $U$  as  $t^2/U$ , passing through a maximum at  $U/2D_{\text{eff}} \sim 1$ .

The review of this and similar results obtained for disordered Hubbard model in DMFT+ $\Sigma$  approximation can be found in [21].

## BASIC RELATIONS FOR THE UPPER CRITICAL FIELD

In Nozieres–Schmitt-Rink approach the critical temperature of superconducting transition is determined by combined solution of the weak coupling equation for Cooper instability in particle–particle (Cooper) channel and the equation for chemical potential for all values of Hubbard interaction within DMFT+ $\Sigma$  procedure. The usual condition for Cooper instability is written as:

$$1 = -U\chi(\mathbf{q}), \quad (7)$$

where  $\chi(\mathbf{q})$  is Cooper susceptibility, determined by the loop diagram in Cooper channel, shown in Fig. 1. In the presence of an external magnetic field total momentum in Cooper channel  $\mathbf{q}$  acquires contribution from the vector potential  $\mathbf{A}$

$$\mathbf{q} \rightarrow \mathbf{q} - \frac{2e}{c} \mathbf{A}. \quad (8)$$

As we assume isotropic electron spectrum, Cooper susceptibility  $\chi(\mathbf{q})$  depends on  $\mathbf{q}$  only via  $q^2$ . The minimal eigenvalue of  $(\mathbf{q} - 2e/c\mathbf{A})^2$ , determining

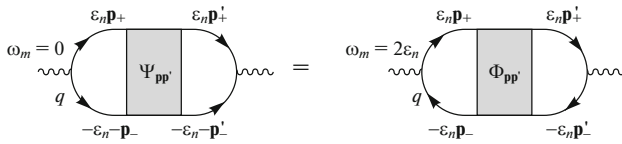


**Fig. 1.** Equivalence of loops in the Cooper and diffusion channels in the case of time inversion invariance.

(orbital)<sup>2</sup> upper critical magnetic field  $H = H_{c2}$  is given by [30]

$$q_0^2 = 2\pi \frac{H}{\Phi_0}, \quad (9)$$

where  $\Phi_0 = ch/2e = \pi\hbar/e$  is magnetic flux quantum. Then the equation for  $T_c(H)$  or  $H_{c2}(T)$  remains the same:

$$1 = -U\chi(q^2 = q_0^2). \quad (10)$$

In the following, we shall neglect relatively weak magnetic field influence on diffusion processes (broken time reversal invariance), which is reflected in non equality of loop diagrams in Cooper and diffusion channels. This influence was analyzed in [9, 10, 31, 32], where it was shown that the account of this broken symmetry only slightly decreases the value of  $H_{c2}(T)$  at low temperatures, even close to the Anderson transition. In the case of time reversal invariance and due the static nature of impurity scattering “dressing” two-particle Green’s function  $\Psi_{\mathbf{p}, \mathbf{p}'}(\varepsilon_n, \mathbf{q})$  we can change directions of all lower electronic lines in the loop with simultaneous sign change of all momenta on these lines (cf. Fig. 1). Then we obtain:

$$\Psi_{\mathbf{p}, \mathbf{p}'}(\varepsilon_n, \mathbf{q}) = \Phi_{\mathbf{p}, \mathbf{p}'}(\omega_m = 2\varepsilon_n, \mathbf{q}), \quad (11)$$

where  $\varepsilon_n$  are Fermionic Matsubara frequencies,  $\mathbf{p}_{\pm} = \mathbf{p} \pm \mathbf{q}/2$ , and  $\Phi_{\mathbf{p}, \mathbf{p}'}(\omega_m = 2\varepsilon_n, \mathbf{q})$  is the two-particle Green’s function in diffusion channel, dressed by impurities. Then we obtain the Cooper susceptibility as:

$$\chi(\mathbf{q}) = -T \sum_{n, \mathbf{p}, \mathbf{p}'} \Psi_{\mathbf{p}, \mathbf{p}'}(\varepsilon_n, \mathbf{q}) \quad (12)$$

$$= -T \sum_{n, \mathbf{p}, \mathbf{p}'} \Phi_{\mathbf{p}, \mathbf{p}'}(\omega_m = 2\varepsilon_n, \mathbf{q}).$$

Performing the standard summation over Fermionic Matsubara frequencies [29, 30] we obtain for Cooper susceptibility entering Eq. (10):

$$\chi(q_0^2) = -\frac{1}{2\pi} \int_{-\infty}^{\infty} d\varepsilon \text{Im} \Phi^{RA}(\omega = 2\varepsilon, q_0^2) \tanh \frac{\varepsilon}{2T}, \quad (13)$$

where  $\Phi^{RA}(\omega, \mathbf{q}) = \sum_{\mathbf{p}, \mathbf{p}'} \Phi_{\mathbf{p}, \mathbf{p}'}^{RA}(\omega, \mathbf{q})$ . To find the loop  $\Phi^{RA}(\omega, \mathbf{q})$  in the case of strong disorder (including the

region of Anderson localization) we use the approximate self-consistent theory of localization [30, 35–40]. Then this loop contains the diffusion pole contribution, which is written as [20]:

$$\Phi^{RA}(\omega = 2\varepsilon, q_0^2) = -\frac{\sum_{\mathbf{p}} \Delta G_{\mathbf{p}}(\varepsilon)}{\omega + iD(\omega)q_0^2}, \quad (14)$$

where  $\Delta G_{\mathbf{p}}(\varepsilon) = G^R(\varepsilon, \mathbf{p}) - G^A(-\varepsilon, \mathbf{p})$ ,  $G^R$  and  $G^A$  are retarded and advanced Green’s functions, while  $D(\omega)$  is frequency dependent generalized diffusion coefficient. As a result, Eq. (10) for  $H_{c2}(T)$  takes the form:

$$1 = -\frac{U}{2\pi} \int_{-\infty}^{\infty} d\varepsilon \text{Im} \left[ \frac{\sum_{\mathbf{p}} \Delta G_{\mathbf{p}}(\varepsilon)}{2\varepsilon + iD(2\varepsilon)2\pi H_{c2}/\Phi_0} \right] \tanh \frac{\varepsilon}{2T}. \quad (15)$$

The generalized diffusion coefficient in self-consistent theory of localization [30, 35–40] for the model under consideration is determined by the following self-consistence equation [20]:

$$D(\omega) = i \frac{\langle v \rangle^2}{d} \left( \omega - \Delta \Sigma_{\text{imp}}^{RA}(\omega) + \Delta^4 \sum_{\mathbf{p}} \Delta G_{\mathbf{p}}^2(\varepsilon) \times \sum_{\mathbf{q}} \frac{1}{\omega + iD(\omega)q^2} \right)^{-1}, \quad (16)$$

where  $\omega = 2\omega$ ,  $\Delta \Sigma_{\text{imp}}^{RA}(\omega) = \Sigma_{\text{imp}}^R(\varepsilon) - \Sigma_{\text{imp}}^A(-\varepsilon)$ ,  $d$  is space dimensionality, while the average velocity  $\langle v \rangle$  is defined here as:

$$\langle v \rangle = \frac{\sum_{\mathbf{p}} |\mathbf{v}_{\mathbf{p}}| \Delta G_{\mathbf{p}}(\varepsilon)}{\sum_{\mathbf{p}} \Delta G_{\mathbf{p}}(\varepsilon)}, \quad \mathbf{v}_{\mathbf{p}} = \frac{\partial \varepsilon(\mathbf{p})}{\partial \mathbf{p}}. \quad (17)$$

Taking into account the limits of diffusion approximation summation over  $q$  in Eq. (16) should be limited by [30, 39]

$$q < k_0 = \min\{l^{-1}, p_F\}, \quad (18)$$

where  $l$  is the mean-free path due to elastic scattering by disorder and  $p_F$  is the Fermi momentum.

In the limit of weak disorder, when localization corrections are small, Cooper susceptibility  $\chi(\mathbf{q})$  is determined by ladder approximation. In this approximation Cooper susceptibility was studied by us in [27]. Let us now rewrite self-consistency Eq. (16) so that in the limit of weak disorder it explicitly reproduces the results of ladder approximation. In this approximation we neglect all contributions to irreducible vertex from “maximally crossed” diagrams and the last term in the r.h.s. of Eq. (16) just vanishes. Now we introduce the

<sup>2</sup> In this paper we do not consider paramagnetic effect due to electronic spin.

frequency dependent generalized diffusion coefficient in ladder approximation as:

$$D_0(\omega) = \frac{\langle v \rangle^2}{d} \frac{i}{\omega - \Delta \Sigma_{\text{imp}}^{RA}(\omega)}. \quad (19)$$

The value of  $\langle v \rangle^2/d$ , entering the self-consistency Eq. (16), can now be expressed via this diffusion coefficient  $D_0$  in ladder approximation. Then the self-consistency Eq. (16) takes the form:

$$D(\omega = 2\varepsilon) = D_0(\omega = 2\varepsilon) \left( 1 + \frac{\Delta^4}{2\varepsilon - \Delta \Sigma_{\text{imp}}^{RA}(\omega = 2\varepsilon)} \times \sum_{\mathbf{p}} \Delta G_{\mathbf{p}}^2(\varepsilon) \sum_{\mathbf{q}} \frac{1}{2\varepsilon + iD(\omega = 2\varepsilon)q^2} \right)^{-1}. \quad (20)$$

In the framework of the approach of [27] the diffusion coefficient  $D_0(\omega = 2\varepsilon)$  in ladder approximation can be obtained in analytic form. In fact, in the ladder approximation, the two-particle Green's function (14) can be written as:

$$\Phi_0^{RA}(\omega = 2\varepsilon, \mathbf{q}) = - \frac{\sum_{\mathbf{p}} \Delta G_{\mathbf{p}}(\varepsilon)}{\omega + iD_0(\omega = 2\varepsilon)q^2}. \quad (21)$$

Let us introduce

$$\begin{aligned} \varphi(\varepsilon, \mathbf{q} = 0) &\equiv \lim_{q \rightarrow 0} \frac{\Phi_0^{RA}(\omega = 2\varepsilon, \mathbf{q}) - \Phi_0^{RA}(\omega = 2\varepsilon, \mathbf{q} = 0)}{q^2} \\ &= \frac{i \sum_{\mathbf{p}} \Delta G_{\mathbf{p}}(\varepsilon)}{\omega^2} D_0(\omega = 2\varepsilon). \end{aligned} \quad (22)$$

Then the diffusion coefficient  $D_0$  can be written as:

$$D_0 = \frac{\varphi(\varepsilon, \mathbf{q} = 0)(2\varepsilon)^2}{i \sum_{\mathbf{p}} \Delta G_{\mathbf{p}}(\varepsilon)}. \quad (23)$$

In [27], using the exact Ward identity, written in ladder approximation, it was shown that  $\varphi(\varepsilon, \mathbf{q} = 0)$  can be expressed as

$$\begin{aligned} \varphi(\varepsilon, \mathbf{q} = 0)(2\varepsilon)^2 &= \sum_{\mathbf{p}} v_x^2 G^R(\varepsilon, \mathbf{p}) G^A(-\varepsilon, \mathbf{p}) \\ &+ \frac{1}{2} \sum_{\mathbf{p}} \frac{\partial^2 \varepsilon(\mathbf{p})}{\partial p_x^2} (G^R(\varepsilon, \mathbf{p}) + G^A(-\varepsilon, \mathbf{p})), \end{aligned} \quad (24)$$

where  $v_x = \partial \varepsilon(\mathbf{p}) / \partial p_x$ .

The procedure for the numerical now looks as follows. First, using Eqs. (24), (23) we find the diffusion coefficient  $D_0$  in the ladder approximation. Then using self-consistency Eq. (20) we find the generalized dif-

fusion coefficient and solve Eq. (15) to determine  $H_{c2}(T)$ .

## MAIN RESULTS

The chemical potential enters Eq. (15) defining  $H_{c2}(T)$  as a parameter, which is to be determined from the condition of band (quarter) filling using the DMFT+ $\Sigma$  procedure. Chemical potential depends not only on the coupling strength, but also on the temperature, and this dependence is quite important in determining the value of  $H_{c2}(T)$  in the limit of strong enough coupling. We use the NRG algorithm as an impurity solver of DMFT neglects electronic levels quantization in magnetic field, i.e., magnetic field influence on electron orbital motion and correspondingly on the chemical potential. In [23] we have shown that in an attractive Hubbard model our DMFT procedure becomes unstable for  $T < T_c$ , which is reflected in finite difference of even and odd iterations of DMFT. This instability is apparently related to instability of the normal state for  $T < T_c$ . In particular, it is most sharp in BEC strong coupling limit (for  $U/2D \geq 1$ ), which makes it impossible to determine the chemical potential at  $T < T_c$ . In the weak coupling limit the difference between the results of even and odd DMFT iterations is very small, which allows us to find the values of  $\mu(T)$  with high accuracy even for  $T < T_c$ . In Fig. 2, we show the temperature dependence of the chemical potential for different values of coupling strength. In the weak coupling limit ( $U/2D = 0.4, 0.6$ ) in Fig. 2 we show data obtained from DMFT+ $\Sigma$  calculations, including the region of  $T < T_c$ . In the limit of strong coupling we can determine the chemical potential directly from DMFT+ $\Sigma$  procedure only at  $T > T_c$  and appropriate data points are also shown in Fig. 2. From Fig. 2, we can see that in the presence of interactions the chemical potential acquires the linear temperature dependence, which is quite important for us. In the weak coupling limit the chemical potential does not have any singularities for  $T < T_c$  and we can assume, that in the strong coupling region  $\mu$  follows the same type of temperature dependence, which can be found from linear extrapolation (dashed lines for  $U/2D = 1.0, 1.4$  in Fig. 2) from the region of  $T > T_c$ . This procedure was used in our calculations for the strong coupling region.

In the limit of weak disorder ( $\Delta/2D = 0.05$  in Fig. 3a) and weak coupling ( $U/2D = 0.2$ ) we observe the temperature dependence of the upper critical field similar to the standard WHH dependence [11] with negative curvature. The growth of the coupling strength in general leads to significant increase of the upper critical field up to extremely high values over  $\Phi_0/2\pi a^2$  ( $a$ —lattice spacing) in the low temperature region. At intermediate couplings ( $U/2D = 0.4, 0.6$ ) the temperature dependence of  $H_{c2}(T)$  acquires weak maximum at  $T/T_c \sim (0.2-0.4)$ . Further increase of the

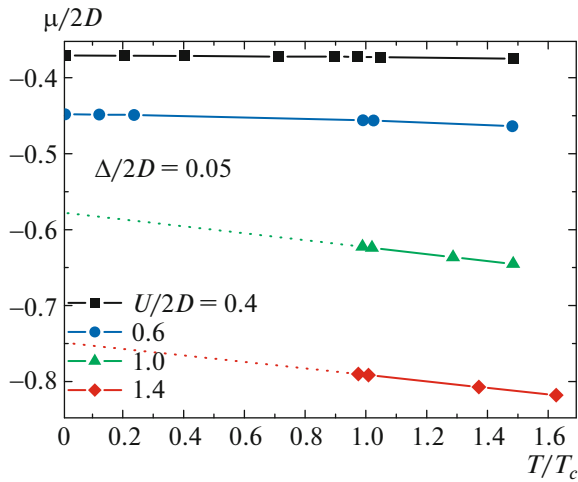


**Fig. 2.** (Color online) Temperature dependences of the chemical potential for  $\Delta/2D = 0.05$  and different values of the interaction.

coupling strength leads to the growth of the upper critical field and for  $U/2D = 1$  the temperature dependence  $H_{c2}(T)$  becomes almost linear and for higher couplings the temperature dependence the value of the upper critical field remains practically the same for all temperatures. With the growth of disorder ( $U/2D = 0.11$  in Fig. 3b), the situation remains qualitatively similar. The increase of the coupling strength leads at first to the growth of  $H_{c2}$  for all temperatures. The small maximum of  $H_{c2}(T)$ , observed at intermediate couplings ( $U/2D = 0.4, 0.6$ ) and weak disorder ( $\Delta/2D = 0.05$ ) vanishes. In the strong coupling region ( $U/2D \geq 1$ )  $H_{c2}(T)$  is in fact linear and only weakly changes with coupling strength. At strong enough disorder ( $\Delta/2D = 0.25$ ) with the growth of coupling strength the upper critical field also grows in the whole temperature region.

This growth continues up to BEC region of very strong coupling ( $U/2D = 1.4$ ), after that  $H_{c2}(T)$  dependence becomes linear and only weakly dependent on the coupling strength. For comparison on the left panel of Fig. 3c for  $U/2D = 0.6$  we show both data obtained using a self-consistent theory of localization (filled triangles and continuous curve) and those calculated from ladder approximation for impurity scattering (unfilled triangles and dashed curve). Weak difference between these dependencies demonstrates that corrections from Anderson localization at this disorder level ( $\Delta/2D = 0.25$ ) are rather weak.

In the model under consideration in DMFT+ $\Sigma$  approximation the Anderson metal–insulator transition occurs at  $\Delta/2D = 0.37$  and this value of critical disorder is independent of the coupling strength (cf. [20]). Temperature behavior of the upper critical field precisely at the point of Anderson transition and in Anderson insulator phase for different values of cou-

pling strength is shown in Fig. 4. In this figure filled symbols and continuous curves show results of calculations using the self-consistent theory of localization, while unfilled symbols and dashed curves correspond to the results of calculations using the ladder approximation for impurity scattering. At the point of Anderson transition ( $\Delta/2D = 0.37$  in Fig. 4a) and in the limit of weak coupling localization effects strongly change the temperature dependence of  $H_{c2}(T)$ . In particular, these effects enhance  $H_{c2}(T)$  in the whole temperature region. However, the greatest increase is observed at low temperatures, so that  $H_{c2}(T)$  dependence acquires positive curvature, as was first shown in [7, 8]. The increase of the coupling strength leads to the growth of the upper critical field in the whole temperature interval. The curves of  $H_{c2}(T)$  in the intermediate coupling region ( $U/2D = 0.6, 1$ ) still have positive curvature. Further increase of the coupling up to  $U/2D = 1.4$  also enhance  $H_{c2}$  at all temperatures. However, the account of localization corrections at such a strong coupling is relevant only at low temperatures ( $T/T_c < 0.1$ ). In this region, the  $H_{c2}(T)$  dependence has positive curvature, while at other temperatures  $H_{c2}(T)$  is, in fact, linear. With further increase of coupling strength ( $U/2D = 1.6$ )  $H_{c2}(T)$  becomes practically linear and localization correction become irrelevant at all temperatures. Thus, in the BEC limit of very strong coupling, the influence of Anderson localization on the behavior of the upper critical field is rather weak. In Anderson insulator phase (Fig. 4b) and in BCS weak coupling limit ( $U/2D = 0.2$ ) the account of localization effects leads to significant growth of  $H_{c2}(T)$  (cf. insert in Fig. 4b). The increase of coupling strength leads to the growth of the upper critical field in the whole temperature region. At intermediate couplings ( $U/2D = 0.6, 1.0$ ) the account of localization effects notably increases  $H_{c2}$  for all temperatures. However, the most significant increase is observed in the region of low temperatures, leading to the positive curvature of  $H_{c2}(T)$  dependence and very sharp growth of  $H_{c2}(T=0)$ . In BEC limit of very strong coupling ( $U/2D = 1.4, 1.6$ ) the upper critical field almost does not grow with coupling strength. Contribution from localization effects for  $T \sim T_c$  is irrelevant and  $H_{c2}(T)$  dependence is practically linear. However, at low temperatures ( $T \ll T_c$ ) contribution from Anderson localization still significantly enhances the upper critical field and  $H_{c2}(T)$  curve has positive curvature. Thus, both in Anderson insulator phase and in BEC limit of very strong coupling the influence of Anderson localization on the behavior of the upper critical field is noticeably suppressed, though at low temperatures it still remains quite significant changing the value of  $H_{c2}(T=0)$ .

In Fig. 5 we show temperature dependencies of the upper critical field for different levels of disorder in three characteristic regions of coupling strength: in



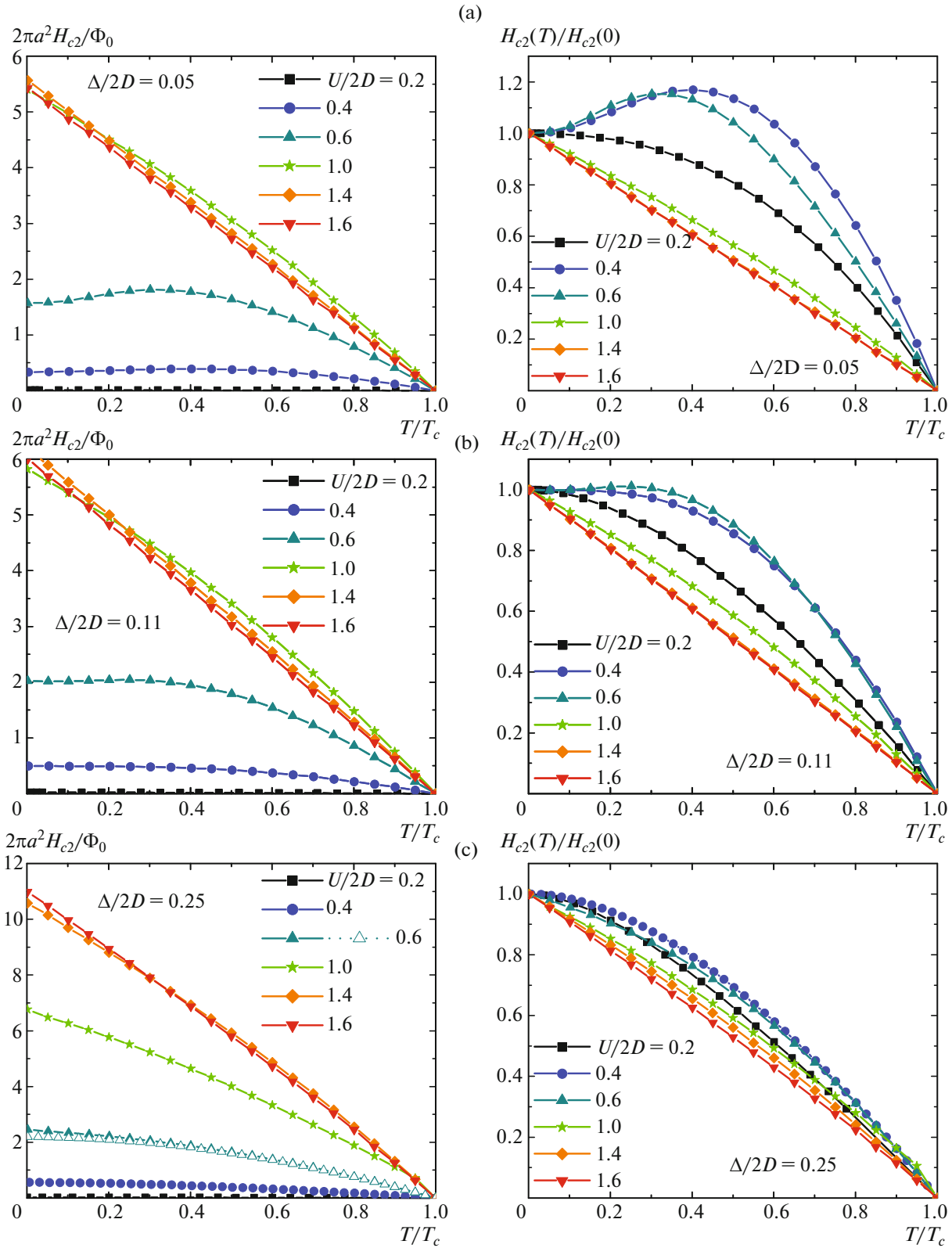


**Fig. 3.** (Color online) Temperature dependences of the upper critical field for different values of the coupling strength for different disorder levels. The upper critical field on the left panels is normalized to  $\Phi_0/(2\pi a^2)$ ; on the right panels, the upper critical field is normalized to its value at  $T = 0$ .

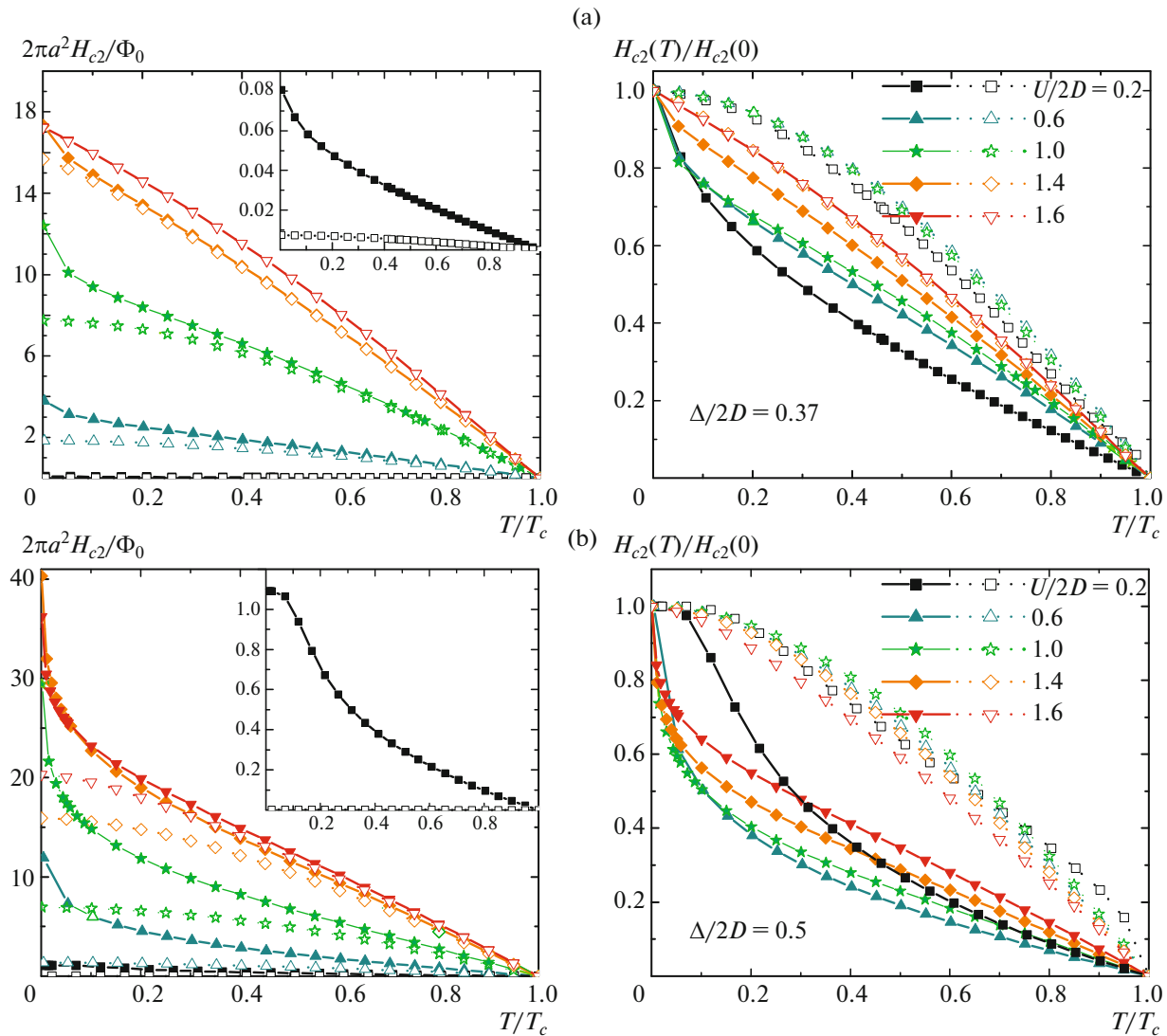


**Fig. 4.** (Color online) Temperature dependences of the upper critical field (a) on the Anderson metal–insulator transition and (b) in the Anderson insulator phase for different values of the coupling strength. On the left panels,  $H_{c2}$  is normalized to  $\Phi_0/(2\pi a^2)$ ; the upper critical field on the right panels is normalized to its value at  $T = 0$ .

BCS weak coupling limit ( $U/2D = 0.2$ ), in BCS–BEC crossover region (intermediate coupling  $U/2D = 1.0$ ) and in BEC limit of strong coupling ( $U/2D = 1.6$ ). In weak coupling limit (Fig. 5a) the growth of disorder leads to the increase of the upper critical field in the whole temperature region in the limit of weak disorder ( $\Delta/2D < 0.19$ ), while the temperature dependence has the negative curvature and is close to the standard WHH dependence [11]. With further increase of disorder with no account for localization corrections, the upper critical field decreases for all temperatures. However, taking into account localization corrections in the weak coupling limit for the case of strong disorder ( $\Delta/2D \geq 0.37$ ) significantly increases the upper critical field and qualitatively changes its temperature dependence, so that the curves of  $H_{c2}(T)$  acquire pos-

itive curvature. The upper critical field rapidly grows with disorder at all temperatures. For intermediate coupling (Fig. 5b) in the limit of weak disorder the temperature dependence of the upper critical field becomes practically linear. The upper critical field grows with disorder at all temperatures. In the limit of strong disorder ( $\Delta/2D \geq 0.37$ ) localization corrections, as in the weak coupling limit, increase the upper critical field at all temperatures and the curves of  $H_{c2}(T)$  acquire positive curvature. However, in the intermediate coupling region the influence of localization corrections is much weaker, than in the weak coupling limit and is relevant only at low temperatures. In BEC limit of the strong coupling (Fig. 5c) and in the limit of weak disorder the curves of  $H_{c2}(T)$  are in fact linear. The upper critical field grows with disorder at all tem-



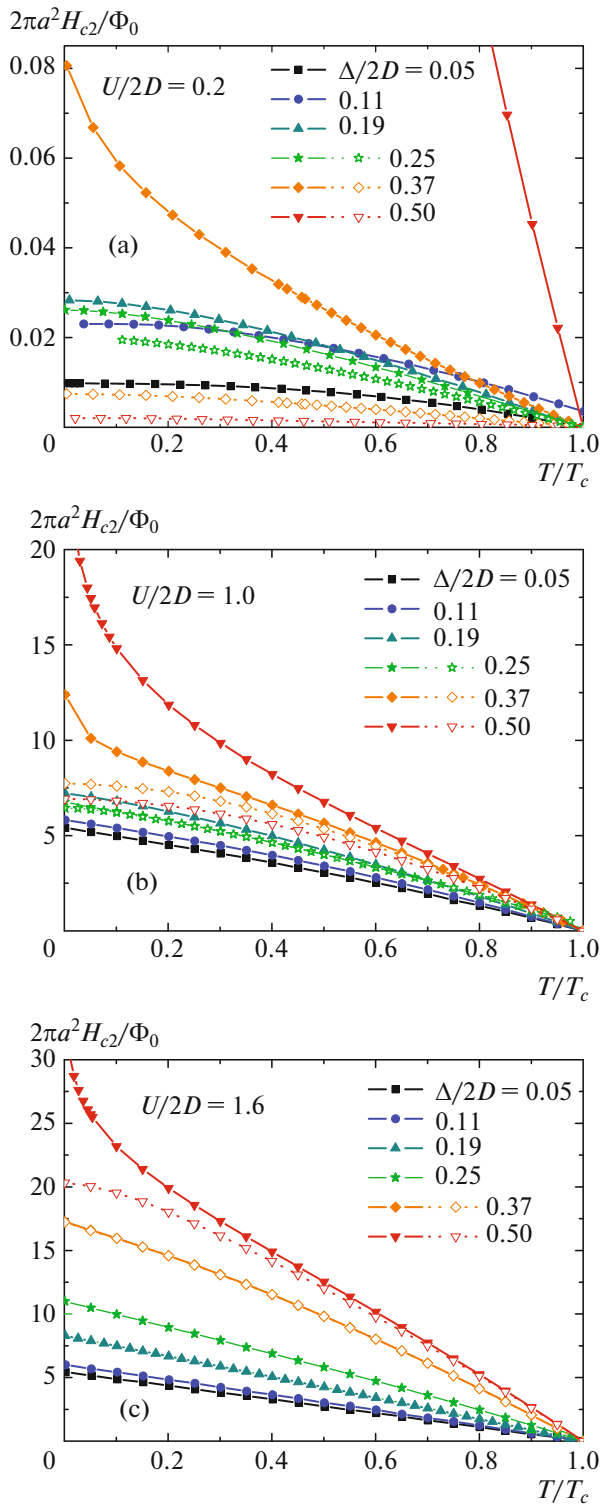


**Fig. 5.** (Color online) Temperature dependences of the upper critical field for different disorder levels: (a) BCS weak coupling limit, (b) BCS–BEC crossover region at intermediate coupling, (c) BEC strong coupling limit. Dark symbols and solid curves correspond to calculations taking localization corrections into account. Light symbols and dashed curves correspond to the ladder approximation for impurity scattering.

temperatures. In the limit of strong disorder at the point of Anderson transition ( $\Delta/2D = 0.37$ ) the  $H_{c2}(T)$  dependence remains linear and the account of localization corrections in fact does not change the temperature dependence of the upper critical field. Further increase of disorder leads to the increase of  $H_{c2}(T)$ . Deeply in the Anderson insulator phase ( $\Delta/2D = 0.5$ ) the  $H_{c2}(T)$  dependence acquires the positive curvature and the account of localization effects enhances  $H_{c2}(T)$  in the low temperature region, while close to  $T_c$  localization corrections are irrelevant even at such a strong disorder. Thus, the strong coupling significantly decreases the influence of localization effects of the temperature dependence of the upper critical field.

## CONCLUSIONS

In this paper, within the combined Nozières–Schmitt-Rink and DMFT+ $\Sigma$  generalization of the dynamical mean field theory we have investigated the influence of disordering, in particular the strong one (including the region of Anderson localization), and the growth of the strength of pairing interaction upon the temperature dependence of the upper critical field. Calculations were performed for the wide range of attractive potentials  $U$ , from the weak coupling limit of  $U/2D \ll 1$ , where instability of the normal phase and superconductivity is well described by BCS model, up to the strong coupling limit of  $U/2D \gg 1$ , where the superconducting transition is due to Bose–Einstein condensation of compact Cooper pairs, which are formed at temperatures much higher than the temperature of superconducting transition.

The growth of the coupling strength  $U$  leads to the fast increase of  $H_{c2}(T)$ , especially at low temperatures. In BEC limit and in the region of BCS–BEC crossover  $H_{c2}(T)$  dependence becomes practically linear. Disordering also leads to the increase of  $H_{c2}(T)$  at any coupling. In the weak coupling BCS limit the growth of disorder increases both the slope of the upper critical field close to  $T = T_c$  and  $H_{c2}(T)$  in low temperature region. In the limit of strong disorder in the vicinity of Anderson transition localization corrections lead to additional sharp increase of the upper critical field at low temperatures and  $H_{c2}(T)$  dependence becomes concave, i.e., acquires positive curvature. In BCS–BEC crossover region and in BEC limit weak disorder is insignificant for the slope of the upper critical field at  $T_c$ , though the strong disorder in the vicinity of Anderson transition leads to noticeable increase of the slope of the upper critical field with the growth of disorder. In the low temperature region  $H_{c2}(T)$  significantly grows with the growth of disorder, especially in the vicinity of Anderson transition, where localization corrections noticeably increase  $H_{c2}(T=0)$  and  $H_{c2}(T)$  curve instead of linear temperature dependence, typical in the strong coupling limit at weak disorder, becomes concave.

In our model, the upper critical field at low temperatures may reach extremely large values significantly exceeding  $\Phi_0/2\pi a^2$ . This makes important the further analysis of the model, taking into account paramagnetic effect and inevitable role of electron spectrum quantization in magnetic field. Actually, we can hope that effects of quantization of the spectrum are irrelevant in the limit of the strong disorder, while paramagnetic effect is much weakened in the region of strong and very strong coupling. These questions will be the task of further studies.

### ACKNOWLEDGMENTS

This work was performed within the State Contract (FASO) no. 0389-2014-0001 with partial support by RFBR grant no. 17-02-00015 and the Program of Fundamental Research of the RAS Presidium “Fundamental problems of high-temperature superconductivity.”

### REFERENCES

1. A. A. Abrikosov and L. P. Gor'kov, *Sov. Phys. JETP* **9**, 220 (1959).
2. A. A. Abrikosov and L. P. Gor'kov, *Sov. Phys. JETP* **9**, 1090 (1959).
3. L. P. Gor'kov, *Sov. Phys. JETP* **36**, 1364 (1959).
4. A. A. Abrikosov and L. P. Gor'kov, *Sov. Phys. JETP* **12**, 1243 (1961).
5. P. W. Anderson, *J. Phys. Chem. Solids* **11**, 26 (1959).
6. P. G. de Gennes, *Superconductivity of Metals and Alloys* (W. A. Benjamin, New York, 1966).
7. L. N. Bulaevskii and M. V. Sadovskii, *JETP Lett.* **39**, 640 (1984).
8. L. N. Bulaevskii and M. V. Sadovskii, *J. Low Temp. Phys.* **59**, 89 (1985).
9. M. V. Sadovskii, *Phys. Rep.* **282**, 226 (1997).
10. M. V. Sadovskii, *Superconductivity and Localization* (World Scientific, Singapore, 2000).
11. N. R. Werthamer and E. Helfand, *Phys. Rev.* **147**, 288 (1966); N. R. Werthamer, E. Helfand, and P. C. Hohenberg, *Phys. Rev.* **147**, 295 (1966).
12. P. Nozieres and S. Schmitt-Rink, *J. Low Temp. Phys.* **59**, 195 (1985).
13. Th. Pruschke, M. Jarrell, and J. K. Freericks, *Adv. Phys.* **44**, 187 (1995).
14. A. Georges, G. Kotliar, W. Krauth, and M. J. Rozenberg, *Rev. Mod. Phys.* **68**, 13 (1996).
15. D. Vollhardt, in *Lectures on the Physics of Strongly Correlated Systems XIV*, Ed. by A. Avella and F. Mancini, *AIP Conf. Proc.* **1297**, 339 (2010).
16. E. Z. Kuchinskii, I. A. Nekrasov, and M. V. Sadovskii, *JETP Lett.* **82**, 198 (2005).
17. M. V. Sadovskii, I. A. Nekrasov, E. Z. Kuchinskii, Th. Prushke, and V. I. Anisimov, *Phys. Rev. B* **72**, 155105 (2005).
18. E. Z. Kuchinskii, I. A. Nekrasov, and M. V. Sadovskii, *Low Temp. Phys.* **32**, 398 (2006); arXiv: cond-mat/0510376.
19. E. Z. Kuchinskii, I. A. Nekrasov, and M. V. Sadovskii, *Phys. Usp.* **53**, 325 (2012); arXiv:1109.2305.
20. E. Z. Kuchinskii, I. A. Nekrasov, and M. V. Sadovskii, *J. Exp. Theor. Phys.* **106**, 581 (2008); arXiv: 0706. 2618.
21. E. Z. Kuchinskii and M. V. Sadovskii, *J. Exp. Theor. Phys.* **122**, 509 (2016).
22. E. Z. Kuchinskii, I. A. Nekrasov, and M. V. Sadovskii, *Phys. Rev. B* **75**, 115102 (2007).
23. N. A. Kuleeva, E. Z. Kuchinskii, and M. V. Sadovskii, *J. Exp. Theor. Phys.* **119**, 264 (2014).
24. E. Z. Kuchinskii, N. A. Kuleeva, and M. V. Sadovskii, *JETP Lett.* **100**, 192 (2014).
25. E. Z. Kuchinskii, N. A. Kuleeva, and M. V. Sadovskii, *J. Exp. Theor. Phys.* **120**, 1055 (2015).
26. E. Z. Kuchinskii, N. A. Kuleeva, and M. V. Sadovskii, *J. Exp. Theor. Phys.* **122**, 375 (2016).
27. E. Z. Kuchinskii, N. A. Kuleeva, and M. V. Sadovskii, *Low Temp. Phys.* **42**, 17 (2017).
28. E. Z. Kuchinskii, N. A. Kuleeva, and M. V. Sadovskii, *J. Exp. Theor. Phys.* **125**, 111 (2017).
29. R. Bulla, T. A. Costi, and T. Pruschke, *Rev. Mod. Phys.* **60**, 395 (2008).
30. E. M. Lifshits and L. P. Pitaevski, *Course of Theoretical Physics, Vol. 9: Statistical Physics, Part 2* (Nauka, Moscow, 1978; Pergamon, New York, 1980), Chap. 5.
31. E. Z. Kuchinskii and M. V. Sadovskii, *Sverkhprovodim.: Fiz., Khim., Tekh.* **4**, 2278 (1991).
32. E. Z. Kuchinskii and M. V. Sadovskii, *Physica C* **185–189**, 1477 (1991).
33. A. A. Abrikosov, L. P. Gor'kov, and I. E. Dzyaloshinskii, *Quantum Field Theoretical Methods in Statistical Physics* (Fizmatgiz, Moscow, 1963; Pergamon, Oxford, 1965).
34. M. V. Sadovskii, *Diagrammatics* (Regulyar. Khaotich. Dinamika, Moscow, Izhevsk, 2010; World Scientific, Singapore, 2006).
35. D. Vollhardt and P. Wölfle, *Phys. Rev. B* **22**, 4666 (1980); *Phys. Rev. Lett.* **48**, 699 (1982).
36. P. Wölfle and D. Vollhardt, in *Anderson Localization*, Ed. by Y. Nagaoka and H. Fukuyama, Vol. 39 of *Springer Series in Solid State Sciences* (Springer, Berlin, 1982), p. 26.
37. A. V. Myasnikov and M. V. Sadovskii, *Sov. Phys. Solid State* **24**, 2033 (1982).
38. E. A. Kotov and M. V. Sadovskii, *Z. Phys. B* **51**, 17 (1983).
39. M. V. Sadovskii, in *Soviet Scientific Reviews – Physics Reviews*, Ed. by I. M. Khalatnikov (Harwood Academic, New York, 1986), Vol. 7, p. 1.
40. D. Vollhardt and P. Wölfle, in *Electronic Phase Transitions*, Ed. by W. Hanke and Yu. V. Kopaev (North-Holland, Amsterdam, 1992), vol. 32, p. 1.